

Plasmonic Films Can Easily Be Better: Rules and Recipes

*Kevin M. McPeak, Sriharsha V. Jayanti, Stephan J. P. Kress,
Stefan Meyer, Stelio Iotti, Aurelio Rossinelli, and David J. Norris**

Optical Materials Engineering Laboratory, ETH Zurich, 8092 Zurich, Switzerland.

*Corresponding author. Email: dnorris@ethz.ch.

Supporting Information

1. Characterization

A. Ellipsometry

A J. A. Woollam V-VASE variable-angle spectroscopic ellipsometer with rotating analyzer was used to determine the optical constants for Cu, Au, and Ag in Figure 4 and the 5 Å/sec deposited Al film in Figure 5 of the main text. Figures S1, S2, S5, S6, and S7 below also used this instrument. Psi and delta values were collected every 10 nm from 400 to 1750 nm at incident angles of 65, 70, and 75 degrees.

A J. A. Woollam VUV-VASE variable-angle spectroscopic ellipsometer with rotating analyzer was used to determine the optical constants for Al in Figure 4 and the 150 Å/sec deposited Al film in Figure 5 of the main text. Psi and delta values were collected every 5 nm from 150 to 1700 nm at incident angles of 65, 70, and 75 degrees.

The complex dielectric functions for Cu, Ag, and Au were determined using the two-phase (substrate-ambient) model:^{S1}

$$\frac{\varepsilon}{\varepsilon_a} = \sin^2 \varphi \left[1 + \tan^2 \varphi \left(\frac{1 - \rho}{1 + \rho} \right)^2 \right]$$

Where ε and ε_a are the complex dielectric functions for the metal and ambient environment, respectively, φ is the angle of incidence, and $\rho = \frac{r_p}{r_s} = \tan(\psi)e^{i\Delta}$. $\frac{r_p}{r_s}$ is the complex reflectance ratio, $\tan(\psi)$ is the amplitude ratio upon reflection, and Δ is the phase difference.

For Al, an aluminum oxide top layer was added to the two-phase model and the oxide thickness was fit via a point-by-point method.

B. Atomic Force Microscopy

A Bruker FastScan atomic force microscope (AFM) was used with a ScanAsyst-Air tip to image grain structure and measure surface roughness for each of our films. The scan area was 2.5 μm x 2.5 μm . Root-mean-squared (RMS) roughness values were extracted using the Gwyddion software package.

2. Fabrication

A. Focused Ion Beam

Metal films were template stripped from silicon templates that had been milled with a FEI Helios focused-ion-beam instrument using 30 kV as the acceleration voltage and 80 pA as the ion-beam current.

B. Template Stripping

Metal films were template stripped using soda lime glass counter-substrates and Norland NOA61 UV epoxy.

2. Supplementary Figures

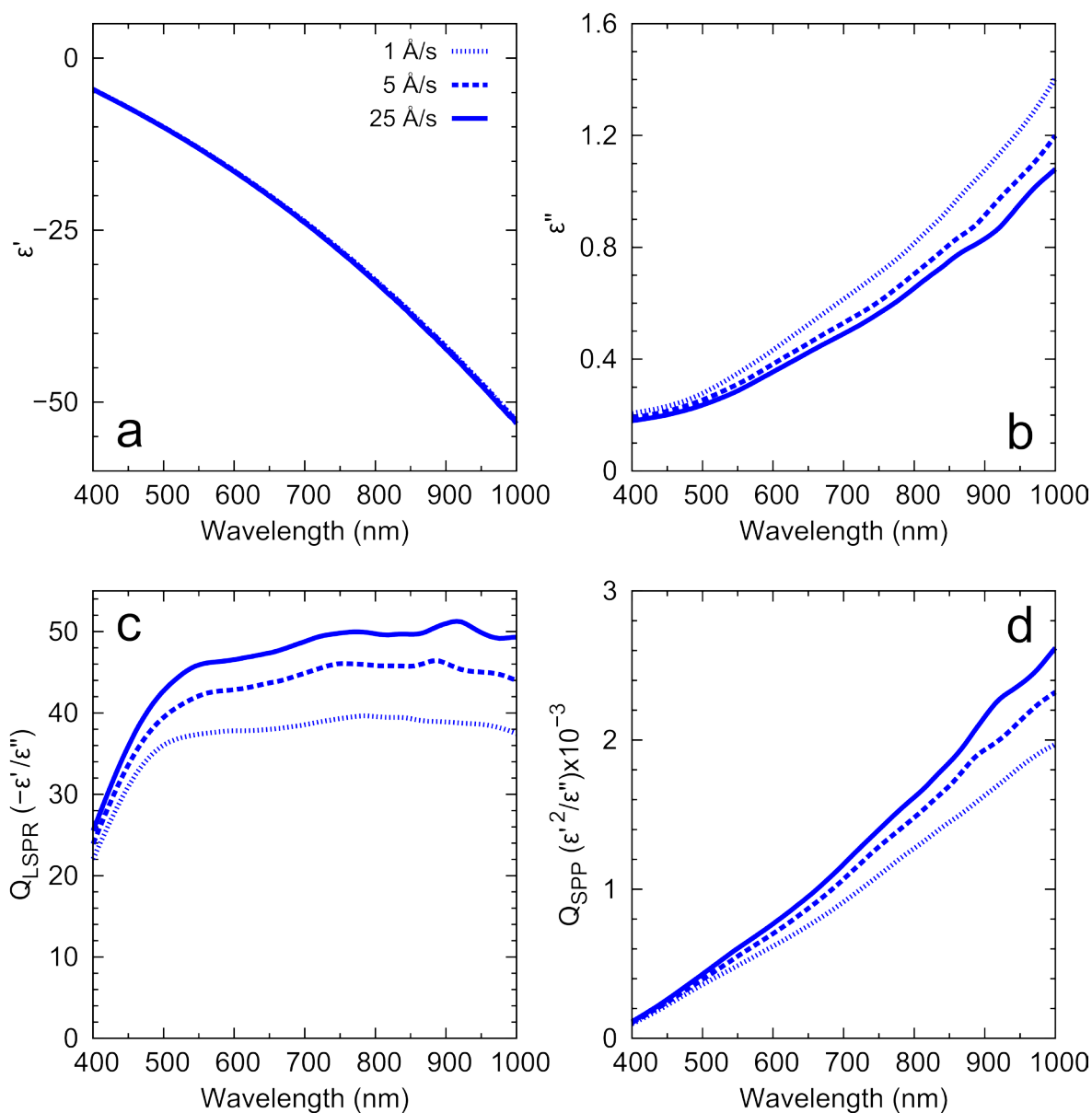


Figure S1. Optical properties and figures-of-merit for the silver template-stripped films shown in Figure 3 of the main text. Films were evaporated at a base pressure of 3×10^{-8} Torr and at rates of 1, 5, and 25 Å/sec. (a) and (b) show the real and imaginary part of the dielectric function, respectively. (c) and (d) plot calculated quality factors^{S2} for the localized surface plasmon resonance in spherical structures (Q_{LSPR}) and surface plasmon polaritons (Q_{SPP}), respectively. The data for the films were smoothed with a five-point moving average.

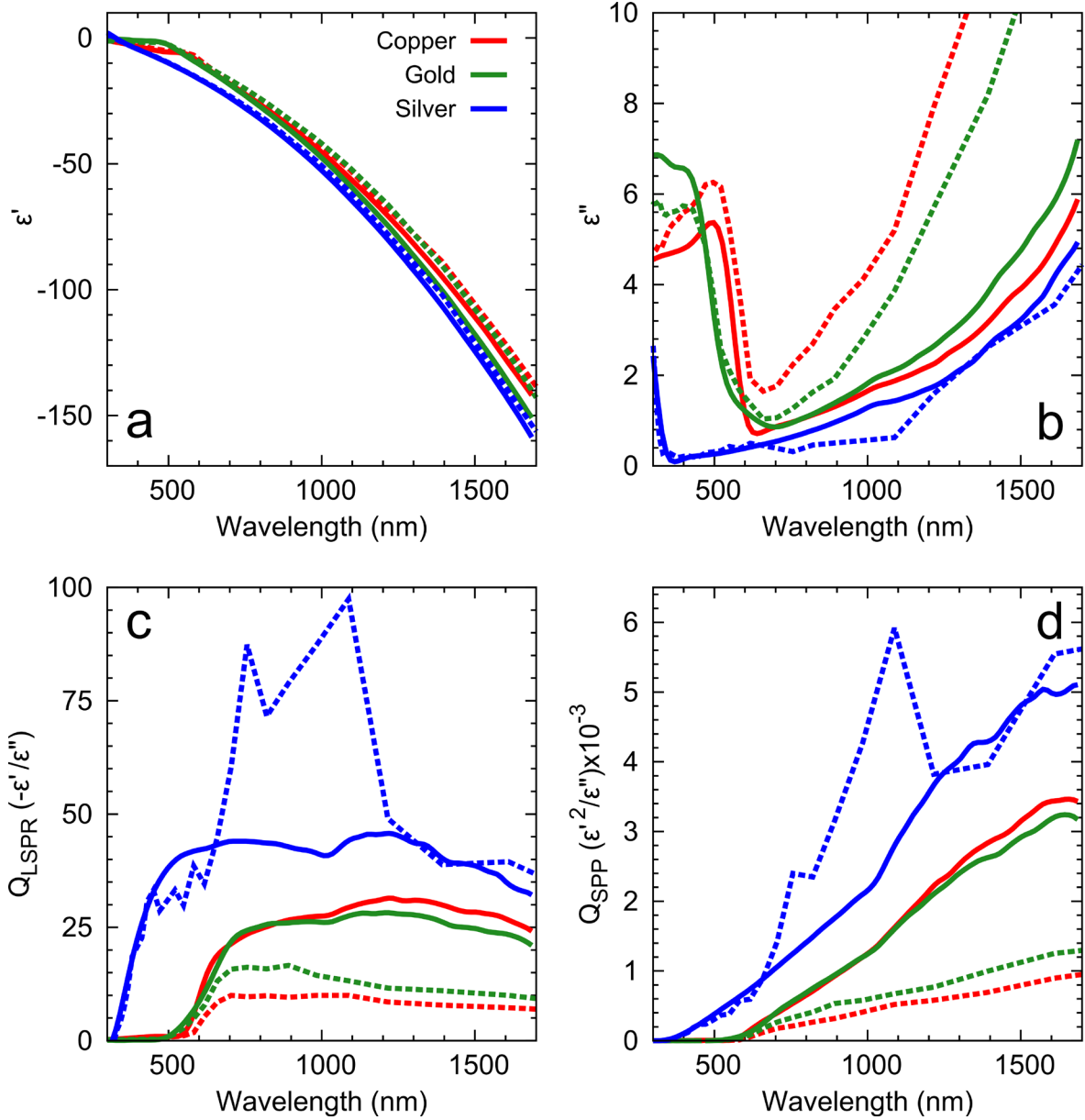


Figure S2. Optical properties and figures-of-merit for copper (red), gold (green), and silver (blue) metal films, as in Figure 3 of the main text. Solid lines are for the recipe films and dashed lines are from Johnson and Christy.^{S3} (a) and (b) show the real and imaginary part of the dielectric function, respectively. (c) and (d) plot calculated quality factors^{S2} for the localized surface plasmon resonance in spherical structures (Q_{LSPR}) and surface plasmon polaritons (Q_{SPP}), respectively. The data for the films were smoothed with a five-point moving average.

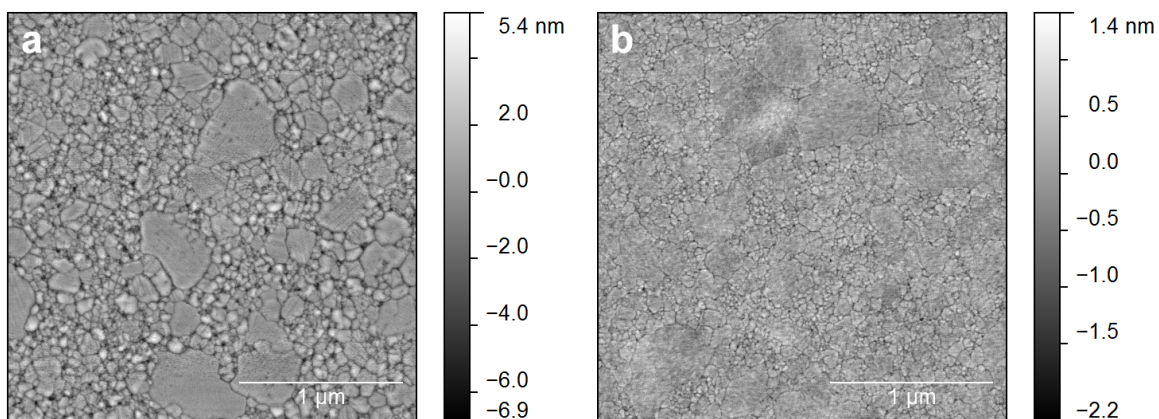


Figure S3. Atomic force micrographs of silver films deposited at $0.2 \text{ \AA}/\text{sec}$ at a base pressure of (a) 3×10^{-6} Torr and (b) 3×10^{-8} Torr. The template-stripped side of the film is shown. The roughness values, calculated over the 2.5 \mu m by 2.5 \mu m area, are (a) 1.23 and (b) 0.32 nm RMS .

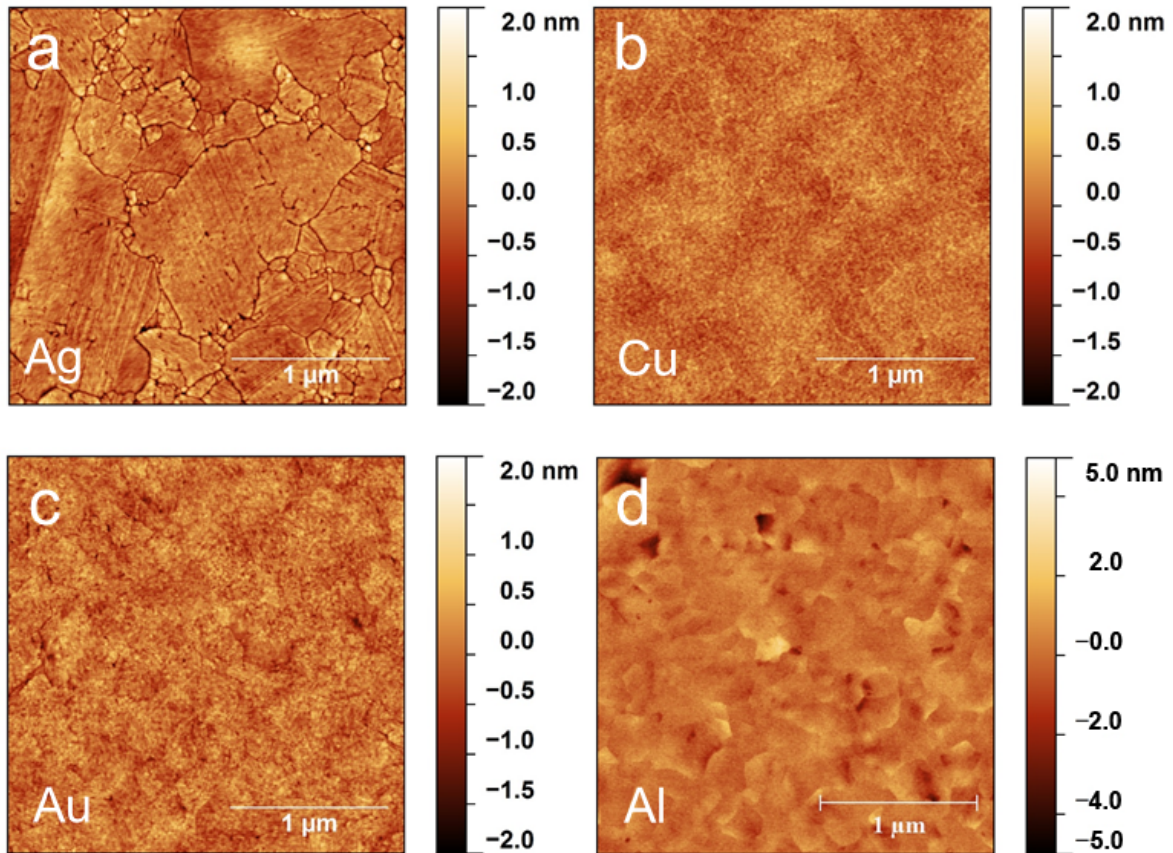


Figure S4. Atomic force micrographs of films deposited at 3×10^{-8} Torr using the rates detailed in Figure 2 in the main text. The template-stripped side of the film is shown. (a) Silver film with 0.37 nm RMS roughness. (b) Copper film with 0.25 nm RMS roughness. (c) Gold film with 0.30 nm RMS roughness. (d) Aluminum film with 0.58 nm RMS roughness. The scan area in each image is $2.5 \mu\text{m}$ by $2.5 \mu\text{m}$.

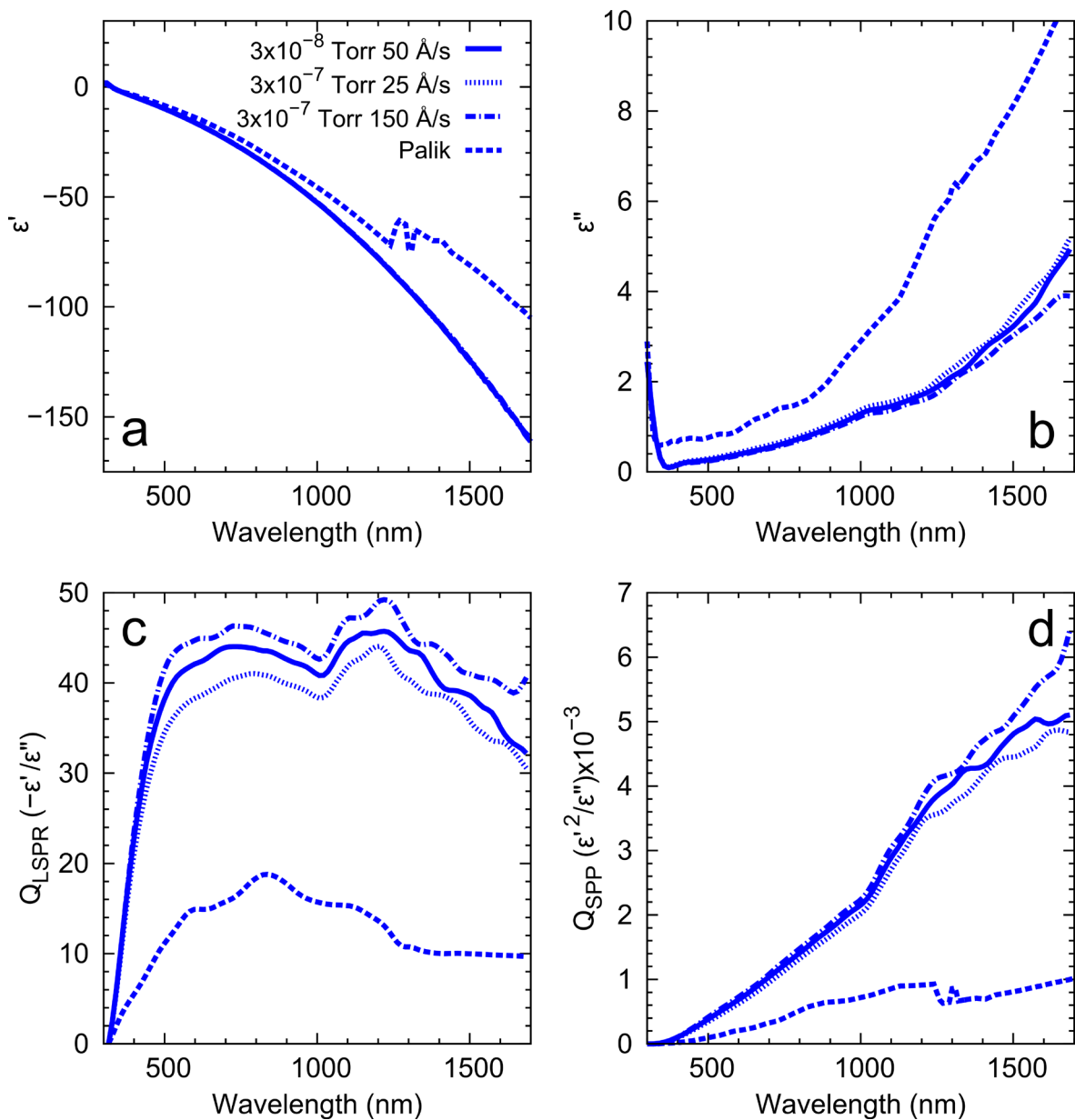


Figure S5. Optical properties and figures-of-merit for silver template-stripped films. A film deposited at a base pressure of 3×10^{-8} Torr and 50 Å/sec (solid lines) is compared with one deposited at 3×10^{-7} Torr and 25 Å/sec (dotted lines) and one deposited at 3×10^{-7} Torr and 150 Å/sec (dash-dotted lines). The dashed lines are from Palik.^{S4} (a) and (b) show the real and imaginary part of the dielectric function, respectively. (c) and (d) plot calculated quality factors^{S2} for the localized surface plasmon resonance in spherical structures (Q_{LSPR}) and surface plasmon polaritons (Q_{SPP}), respectively. The data for the films were smoothed with a five-point moving average.

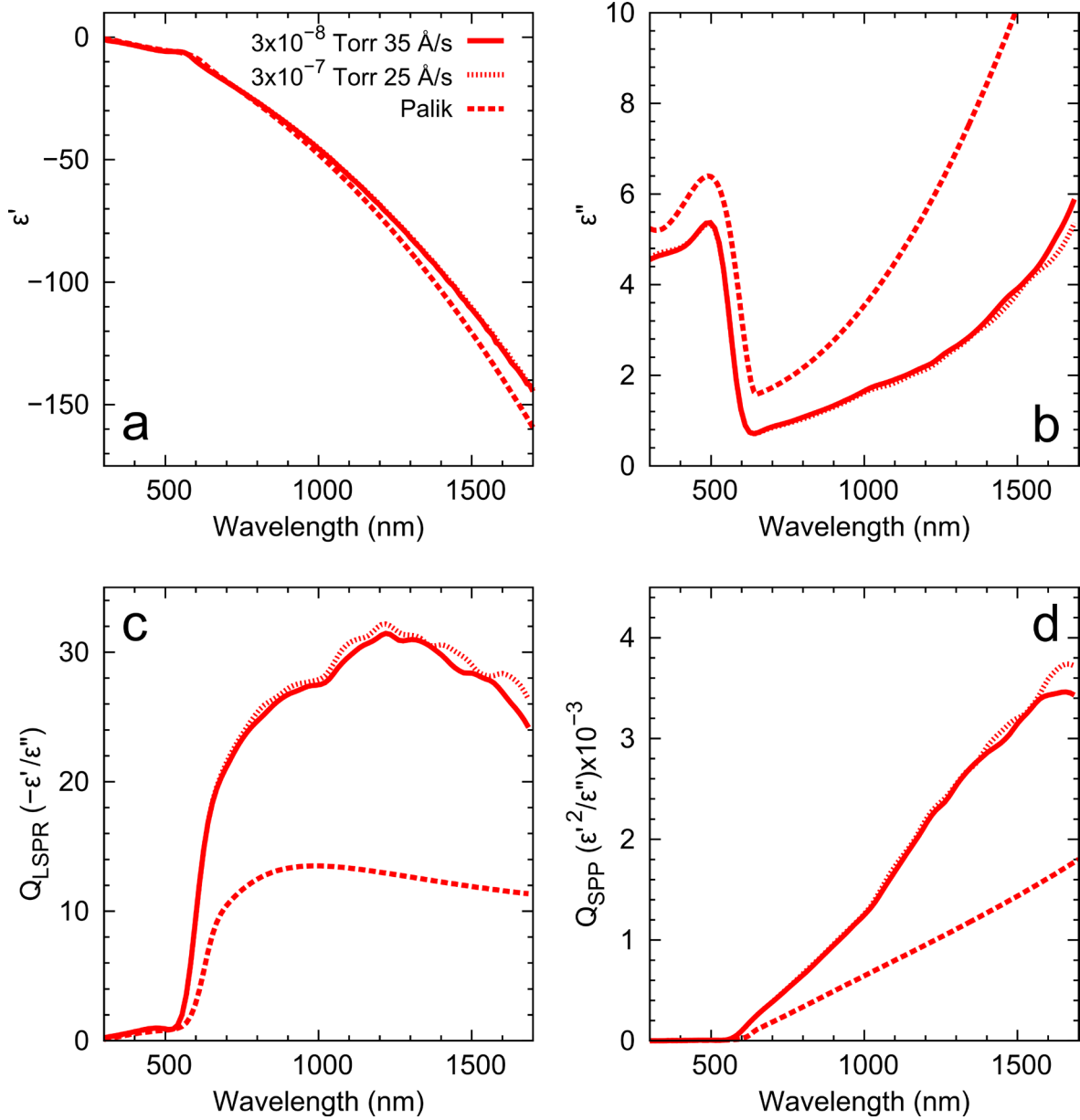


Figure S6. Optical properties and figures-of-merit for copper template-stripped films. A film deposited at a base pressure of 3×10^{-8} Torr and 35 Å/sec (solid lines) is compared with one deposited at 3×10^{-7} Torr and 25 Å/sec (dotted lines). The dashed lines are from Palik.^{S4} (a) and (b) show the real and imaginary part of the dielectric function, respectively. (c) and (d) plot calculated quality factors^{S2} for the localized surface plasmon resonance in spherical structures (Q_{LSPR}) and surface plasmon polaritons (Q_{SPP}), respectively. The data for the films were smoothed with a five-point moving average.

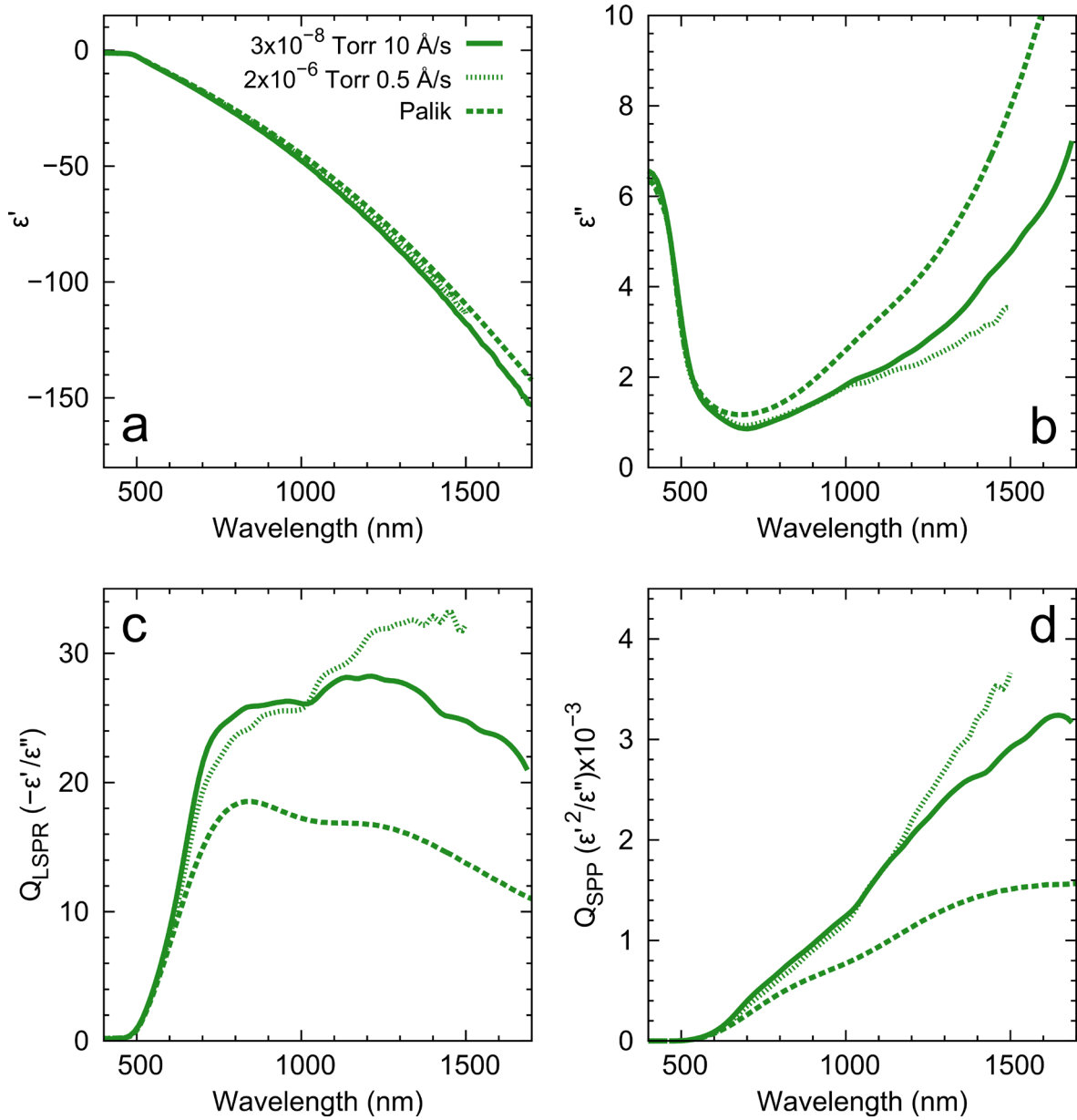


Figure S7. Optical properties and figures-of-merit for gold template-stripped films. A film deposited at a base pressure of 3×10^{-8} Torr and 10 Å/sec (solid lines) is compared with one deposited at 2×10^{-6} Torr and 0.5 Å/sec (dotted lines). The dashed lines are from Palik.^{S4} (a) and (b) show the real and imaginary part of the dielectric function, respectively. (c) and (d) plot calculated quality factors^{S2} for the localized surface plasmon resonance in spherical structures (Q_{LSPR}) and surface plasmon polaritons (Q_{SPP}), respectively. The data for the films were smoothed with a five-point moving average.

3. Supporting References

- S1. Aspnes, D. E., Chapter 5 - The Accurate Determination of Optical Properties by Ellipsometry. In *Handbook of Optical Constants of Solids*, Palik, E. D., Ed. Academic Press: Burlington, 1997; pp 89-112.
- S2. Blaber, M. G.; Arnold, M. D.; Ford, M. J. *J. Phys.-Condes. Matter* **2010**, *22*, 143201.
- S3. Johnson, P. B.; Christy, R. W. *Phys. Rev. B* **1972**, *6*, 4370-4379.
- S4. Palik, E. D., *Handbook of Optical Constants of Solids*. Academic Press: Burlington, 1997.